Slow stable crack growth in high density polyethylenes

M. K. V. Chan and J. G. Williams
Department of Mechanical Engineering, Imperial College of Science and Technology, London SW7 2BX, UK
(Received 19 March 1982)

The phenomenon of slow stable crack growth in polyethylene is investigated using notched specimens subject to constant load and the concepts of fracture mechanics. The effect of specimen geometry and dimension, the loading and the mode of loading on the applied stress intensity factor *versus* crack speed (K_c-$\dot{a}$) curves has been studied to demonstrate that K_c is the controlling stress parameter for crack growth under suitable conditions. K_c-$\dot{a}$ curves are obtained for a high density polyethylene homopolymer in distilled water and in a diluted detergent solution at four different temperatures. Results are also obtained for a much tougher medium density polyethylene copolymer whenever possible. Several mechanisms can be identified from the form of the K_c-$\dot{a}$ curves. Two, in particular, have been observed but not explained before: (i) crack growth with a time dependence of 0.25, and (ii) the high K_c-$\dot{a}$ slopes for crack growth in a tough copolymer. With the help of scanning electron microscopic studies of the fracture surfaces, (i) is postulated to be due to diffusion controlled void growth process and (ii) is considered to be the result of crack tip blunting effects. From the temperature dependence of crack growth, the activation energy of the diffusion controlled crack growth process is found to coincide with that of the α-relaxation process in polyethylene implying that diffusion controlled crack growth may be related to the motion of main chains in the polymer.

Keywords Environmental stress cracking; crack growth; polyethylene; fracture mechanics; fracture surfaces; mechanism

INTRODUCTION

Slow crack propagation in polymers is of considerable practical importance since it occurs at low stresses and can be the cause of long-term failures in engineering components. The presence of active environments can promote this process with crack growth occurring at even lower stresses. A suitable method for characterizing this type of fracture is necessary to understand the basic mechanisms involved and to aid in designing components against long-term failures. In many cases of long-term failures, crack growth initiates from an inherent flaw in the material and extends as a single macroscopic crack until final failure. For a K-increasing test specimen subject to constant load, the whole process from the application of the load to ultimate failure can be broadly divided into four different stages: (a) an incubation period from the application of the load to the initiation of crack growth, (b) a period of 'unsteady' crack growth following crack initiation (this is manifested by non-unique K_c–$\dot{a}$ curves at different starting values of initial K), (c) crack growth which is characterized by a unique K_c–$\dot{a}$ curve (hereinafter, referred to as 'steady' crack growth), and (d) final instability (*Figure 1*). In the widely used test of measuring stress (or some equivalent parameter, e.g. initial stress intensity factor) against time to failure, the four stages are not separated and each stage contributes its proportion to the final failure time. In order to deepen our understanding of the mechanisms involved, it is important to be able to separate the different stages and to consider them separately. This has been made possible with the use of the concepts of fracture mechanics, by monitoring the behaviour of a single artificially-made sharp crack continually. Using such an approach, this paper sets out to investigate the 'steady' crack growth behaviour (stage (c)) of polyethylene. The applicability of fracture mechanics will be demonstrated. The effects of different environments and elevated temperatures on two grades of polyethylene will also be studied and, finally, with the help of fractographic studies, a discussion of possible mechanisms will be made.

FRACTURE MECHANICS CONCEPTS

Fracture mechanics seeks to establish a suitable parameter to characterize the fracture of a cracked body under load. In linear elastic fracture mechanics (LEFM), a single parameter K, the stress intensity factor, is sufficient to relate the intensity of the elastic stress–strain field near the crack tip to the loading and geometry of the body. It has been demonstrated experimentally that a critical value of K, termed K_c, is a suitable criterion for fracture in polyethylene[1], provided the plastic zone size adjacent to the crack tip is small compared to the relevant specimen dimensions of crack length, thickness and width. Under such conditions, K_c is reasonably geometry and loading independent. The mode of loading also influences the validity requirements, e.g. the requirements are less stringent for a higher degree of constraint mode such as bending. The easiest way to demonstrate that fracture is K-controlled is by performing fracture experiments of

0032-3861/83/020234-11$03.00

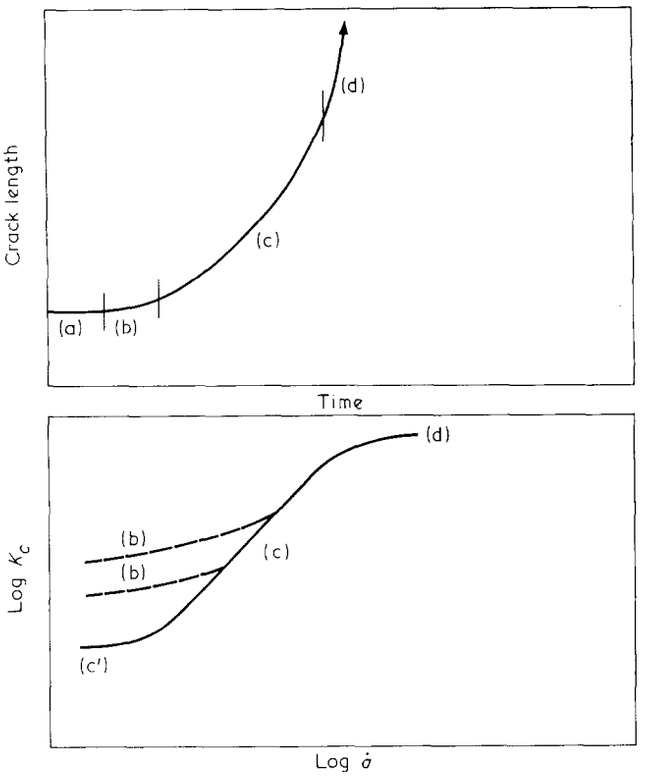

Figure 1 Different stages in long-term failure process of a constant load K-increasing test, and how they are manifested on a K_c–$\dot{a}$ curve: (a) incubation period, (b) 'unsteady-state' behaviour, (c) 'steady-state' behaviour, (c') threshold 'steady-state' behaviour, and (d) instability behaviour. Broken lines represent two different starting values of K_c

different specimen geometries, specimen dimensions, loadings and modes of loading and obtaining K_c values that are independent of each of these parameters.

K can be calculated for different geometries of finite width under different loading conditions using appropriate expressions (e.g. Brown and Srawley[2]). It is usually written as:

$$K = Y\sigma\sqrt{a} \tag{1}$$

where Y = geometric correction factor
σ = gross applied stress
and a = crack length

In time-dependent slow stable crack growth, K_c, although load and geometry independent under valid conditions, depends on the rate of the process as well as external conditions such as temperature and environment. For a given temperature and environment, it is convenient to express the rate dependence of K_c in a power-law form as[3]:

$$K_c \propto \dot{a}^n \tag{2}$$

where $\dot{a}$ = crack speed
and n = measure of the degree of time dependence of the particular process operating.

If equation (2) is applicable, a plot of K_c *versus* $\dot{a}$ on a logarithmic basis will be a straight line.

EXPERIMENTAL

Two grades of polyethylene were used: a high density polyethylene homopolymer of density 960 kg m^{-3} and melt flow index 0.6 g/10 min* (BP Rigidex 006-60) and a tougher medium density polyethylene copolymer of density 940 kg m^{-3} and melt flow index 0.2 g/10 min* (BP Rigidex 002-40). They were supplied in the form of compression moulded sheets of thicknesses of 3, 6, 12 and 20 mm. Rigidex 006-60 cracks more readily and was used as the model material for most of the tests. Tests were extended to 002-40 whenever applicable since this grade is very resistant to crack growth.

Crack growth tests were performed with single-edge notched three-point bend specimens (*Figure 2*). The initial notches were prepared by forming saw-cut slots which were then sharpened with a razor blade. Great care was necessary when sharpening the notch because each notch has to be sharpened with a fresh razor blade. The three-point bend rig has a span of 120 mm and the specimens were subjected to dead loads. Tests were carried out in air, distilled water and a detergent environment (2% Comprox 2740 and 98% distilled water by volume) at temperatures of +19°C (room temperature), +40°C, +60°C and +75°C. At +19°C, the specimens and liquid environments were enclosed in sealed polyethylene bags. At higher temperatures, the whole rig and specimen were immersed in a tank containing the environment whose temperature was controlled by recirculating hot water through copper tubing from a water heater. Water lost through evaporation from the tank was replenished by distilled water from a reservoir admitted through a solenoid valve, whenever necessary, which was controlled by a level control switch monitoring the level of the liquid in the tank. The crack tip was observed with a travelling

* 2.16 kg load, BS3412: 1976

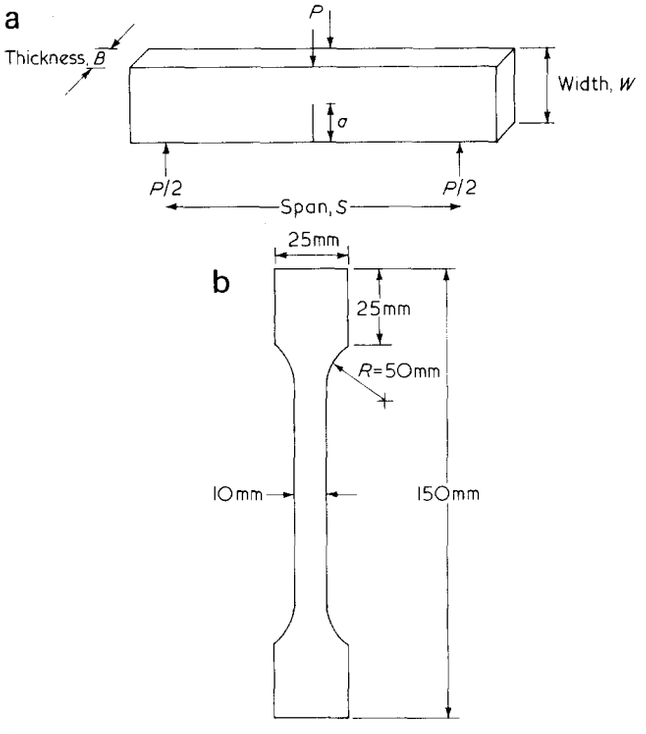

Figure 2 (a) Single-edge notched three-point bend crack growth test specimen. (b) Dumbell creep/yield test specimen

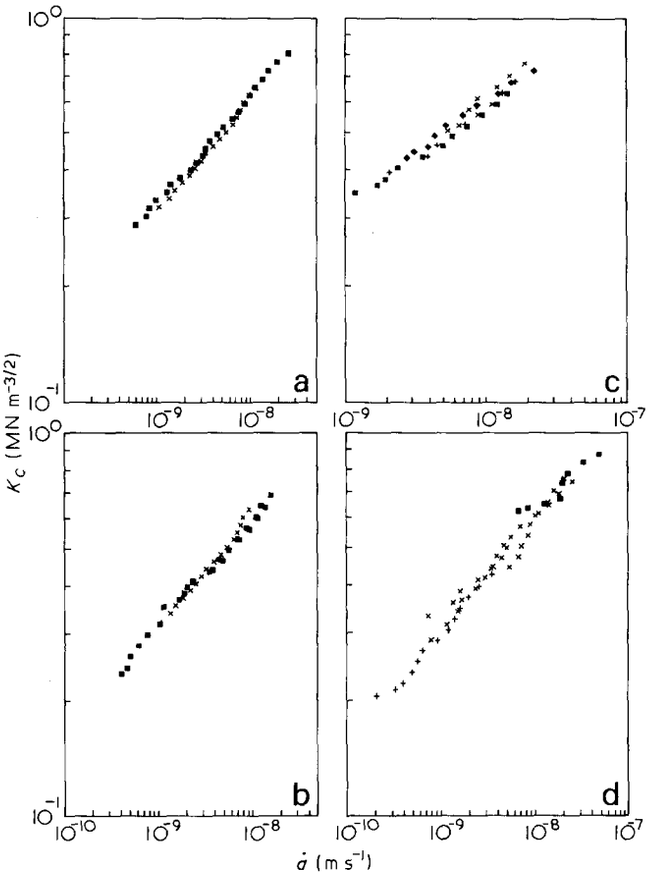

Figure 3 Effect of geometry dimensions and loading on K_c–$\dot{a}$ curves for 006–60 in Comprox 2% at +19°C, SEN three-point bend specimens: (a) effect of thickness B, (■) 12 mm; (x) 6 mm (b) effect of width W, (■) 20 mm; (x) 30 mm (c) effect of initial crack length a_0, (■) 3 mm; (+) 4 mm; (♦) 5 mm; (x) 6 mm and (d) effect of load (in kg) P, (■) 20; (x) 10; (+) 6

binocular microscope (× 35 eyepiece) and crack length measurements could be made at suitable time intervals to an accuracy of ±0.01 mm.

Fracture surfaces were gold-sputtered and examined in a JEOL JSM-T200 scanning electron microscope.

Creep modulus and yield stress data were obtained from dumbell specimens cut from the 3 mm thick compression moulded sheets to the dimensions shown in *Figure 2*. Constant load and constant strain rate tests were performed on an Instron Universal testing machine in air at temperatures corresponding to those used for the crack growth tests. Strains were measured with an Instron extensometer.

RESULTS AND DISCUSSION

Establishing K_c *as the controlling stress parameter for crack growth*

Firstly, it is important to establish that K_c is indeed an appropriate parameter for studying crack growth. This means that a unique K_c–$\dot{a}$ curve for a particular temperature and environment must be obtained that is independent of the specimen geometry, dimensions and loading conditions. Tests were performed on 006-60 to investigate the effects of these parameters on the K_c–$\dot{a}$ curve. From the measured crack length *versus* time curves, the crack speed $\dot{a}$ was found graphically and K_c was calculated from the corresponding a, load and specimens dimensions using equation (1).

It is important to note that in all the crack growth tests, the four different stages of crack incubation, 'unsteady' crack growth, 'steady' crack growth and final instability were observed. The data for K_c–$\dot{a}$ curves in this study refer only to 'steady' crack growth. Typically, this means ignoring the K_c–$\dot{a}$ data for the initial period of crack growth which manifest the type of non-uniqueness shown as region (b) in the K_c–$\dot{a}$ schematic of *Figure 1*.

Figure 3 shows the effect of thickness B, width W, initial crack length a_0 and load P on the K_c–$\dot{a}$ curve for three-point bend specimens of 006-60 in Comprox 2% environment at +19°C. Within the experimental scatter, a unique K_c–$\dot{a}$ curve was obtained in each case. *Figure 4* shows the data for two different modes of loading: SEN three-point bend and SEN tension for 006-60 in distilled water at various temperatures. The SEN tension data were reproduced from work done at BP Chemicals Limited, which have been reported in reference 4. The results can be seen to superimpose on the same curves, although the ratio of the net section stresses for the two modes of loading was found to be approximately:

$$\frac{\sigma_t}{\sigma_b} = 0.2 \qquad (3)$$

where $\sigma_t = P/(B(W-a))$, uniform net section stress for tension and $\sigma_b = (1.5\,P(\text{span}))/(B(W-a)^2)$, nominal stress at the crack tip for bending.

These results and others not reported here demonstrated that the crack speed was indeed controlled by K for the size of specimens examined. It must be pointed out that this may not be true for specimens whose sizes are substantially different (smaller) from these. Moreover, much tougher materials would require bigger specimens[1].

Having established that 'steady' crack growth was K-controlled, subsequent tests were performed on suitably

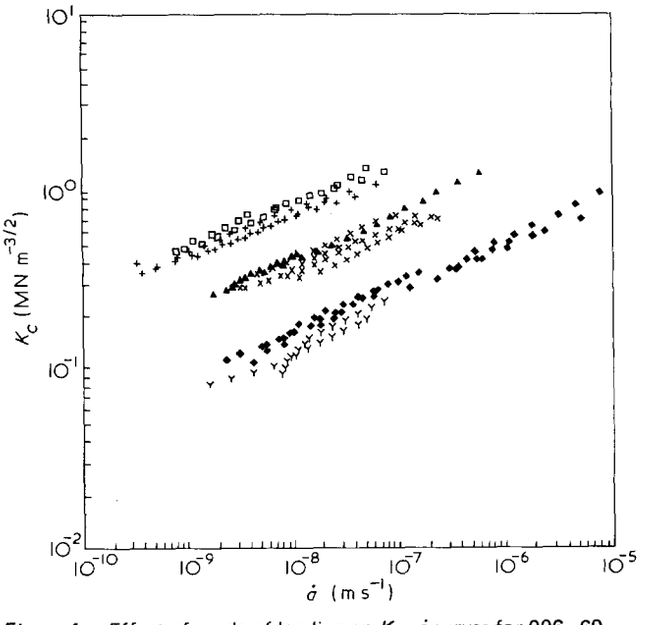

Figure 4 Effect of mode of loading on K_c–$\dot{a}$ curves for 006–60 in distilled water at different temperatures. SEN three-point bend specimens: (□) +19°C; (▲) +40°C; (♦) +75°C. SEN tension specimens: (+) +23°C; (x) +40°C; (Y) + 80°C

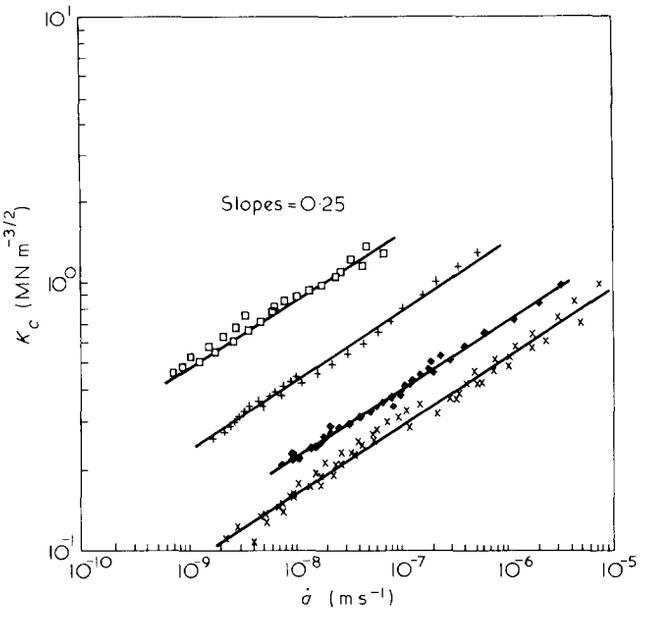

Figure 5 K_c–$\dot{a}$ curves for 006–60 in distilled water at different temperatures: (□) +19°C; (+) +40°C; (♦) +60°C; (x) +75°C

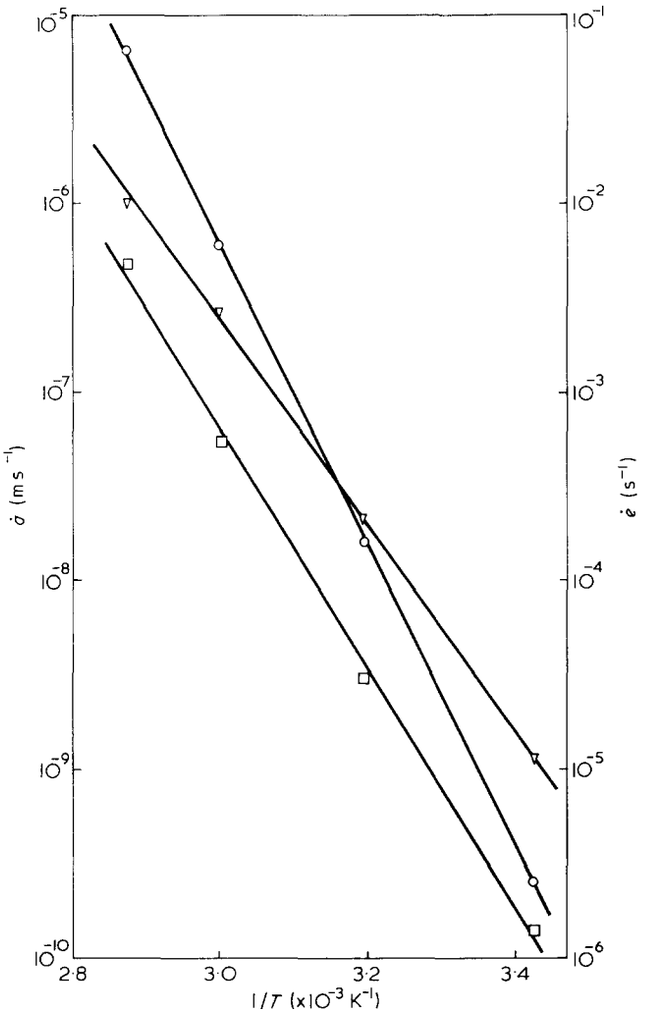

Figure 6 Arrhenius plots for 006–60: (▽) crack growth rate in distilled water, determined at K_c = 0.5 MN m$^{-3/2}$; (□) crack growth rate in Comprox 2%, determined at K_c = 0.2 MN m$^{-3/2}$; (○) strain rate in air, determined at σ_y = 15.85 MN m^{-2}

sized SEN three-point bend specimens, mainly of dimensions of $B = 6$ mm, $W = 30$ mm, $a_0 = 5$ mm and a span of 120 mm.

Effect of temperature on 'steady' crack growth in 006-60 in distilled water

Figure 5 shows the results obtained at four different temperatures. At each temperature, the data fall on a straight line of slope 0.25. The occurrence of this slope will be discussed later in the paper. The temperature dependence can be described by the Arrhenius form of a thermal activated process[3]:

$$K_c = A\,\dot{a}^n\, e^{n(\Delta H/RT)} \tag{4}$$

where A = constant
ΔH = activation energy of the process
R = gas constant
and T = absolute temperature

An Arrhenius plot of ln $\dot{a}$ *versus* $1/T$ at a constant K_c should be a straight line whose slope equals $\Delta H/R$, from which the activation energy ΔH can be determined. *Figure 6* shows such a plot. A straight line is obtained as predicted and the activation energy ΔH is found to be 105 kJ mol^{-1} which coincides with that for the α-relaxation process[5]. The α-relaxation is attributed to vibrational or reorientational motion of the main chain within the polyethylene crystals.

Effect of aggressive environment (Comprox 2%) on 'steady' crack growth in 006-60 at different temperatures

Figure 7 shows the K_c–$\dot{a}$ data in Comprox 2% at four temperatures. At each temperature, not all the data fall on a single straight line and there appears to be a threshold value of K, below which no appreciable crack growth can be observed in 1000 h. Although only data at +19°C and +75°C were obtained near threshold K levels, it is expected that similar behaviour can be observed at the

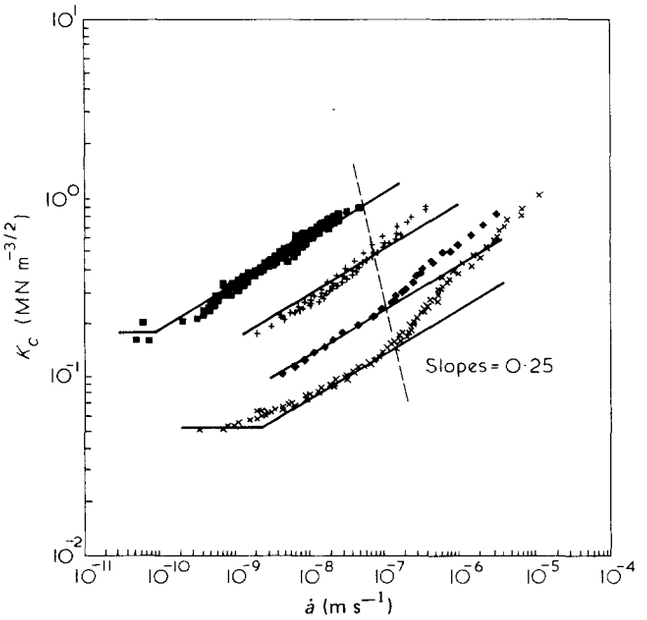

Figure 7 K_c–$\dot{a}$ curves for 006–60 in Comprox 2% at different temperatures: (■) +19°C; (+) +40°C; (♦) +60°C; (x) +75°C. Dotted line shows the transition to flow-controlled crack growth

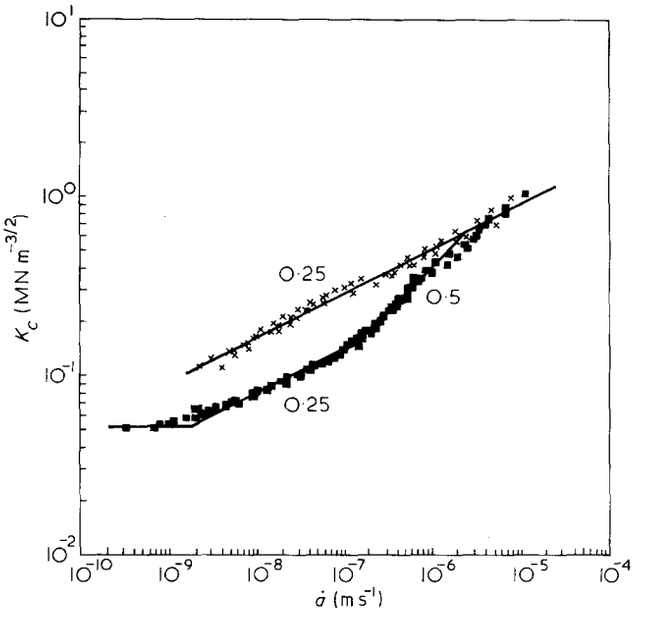

Figure 8 K_c–$\dot{a}$ curves for 006–60 in two different environments at +75°C: (x) distilled water; (■) Comprox 2%. Numbers alongside curves indicate slopes of respective lines

other temperatures (and in distilled water as well). Even if there is not a distinct cut-off as shown in the figure, there is certainly a levelling of the curve in that regime. More data would have to be gathered to ascertain the behaviour near threshold values of K. Some of the data fall on the lines drawn at a slope of 0.25. At higher crack speeds, the data depart to the left of these lines. These observations suggest that various controlling mechanisms may be operating, the contribution of each depends on the speed of the growing crack. The nature of these mechanisms can be seen more clearly by comparing the data in Comprox 2% with those in distilled water, as shown in *Figure 8*, for data at +75°C. It is worth noting that tests at +19°C in distilled water and in air gave similar K_c–$\dot{a}$ curves showing that distilled water may be considered as an inert environment. This is assumed to be true also at higher temperatures. From *Figure 8*, it can be seen that the data in Comprox 2% which fall on the line of slope of 0.25 have the same slope as those in distilled water but are depressed by a certain amount. This indicates that the rate determining process may be the same in both cases but the effect of the detergent is to plasticize the crack tip region causing the depression as observed. The temperature dependence of the process can be described by equation (4), as shown in *Figure 6*, and an activation energy ΔH of 122 kJ mol^{-1} is obtained.

At higher crack speeds, the data depart from the rate dependence of 0.25 and fall on a line of slope of 0.5. As the crack speed increases further, the data in Comprox 2% merge with those in distilled water. This suggests that the departure may be attributed to the effect of incomplete plasticization of the crack tip region by the detergent, proceeding to little or no plasticization as the data in the detergent and in distilled water merge together. The exact nature of this incomplete plasticization is not entirely certain. The slope of 0.5 has been noted before[6] which was attributed to flow-controlled crack growth in which the flow of the environment into the porous crack tip region to effect plasticization was the limiting factor. A transition speed can be defined at the point of departure, as shown by the dotted line in *Figure 7*. It can be seen that the transition speed increases as the test temperature is increased. This may be due to the decrease in viscosity of the liquid as the temperature is increased. *Figure 9* shows the transition speeds as a function of the liquid viscosity. Williams and Marshall[6] have observed an inverse proportionality between the transition speed and the liquid viscosity. Good agreement is obtained with the present results, as shown by the line of slope of −1 in *Figure 9*.

'Steady' crack growth in 002-40 in different environments at various temperatures

The 002-40 grade is extremely resistant to crack growth. At room temperature (+19°C), the fracture toughness of 002-40 measured with the J-integral is about 5 MN m$^{-3/2}$ (ref 7) compared with about 1 MN m$^{-3/2}$ for 006-60.[1] At +19°C, in Comprox 2%, it is possible to produce 'steady' crack growth at K values as low as 0.5 MN m$^{-3/2}$ but crack growth is extremely slow (about 10^{-11} m s^{-1}). One specimen has been under load for almost two years and the crack has extended only about 5 mm. However, substantial crack growth was obtained in Comprox 2% at elevated temperatures. *Figure 10* shows the results obtained so far. The data for distilled water at +80°C were reproduced from reference 4, which have been obtained from SEN tension specimens. Crack growth data in distilled water have not been possible with SEN three-point bend specimens due to buckling difficulties and specimen size limitations. Even the SEN tension data may not be completely satisfactory. From *Figure 10*, it can be seen that the data for 002-40 are much more difficult to interpret. In Comprox 2%, a substantial amount of crack growth at +60°C and +75°C occur with a time dependence of 0.25. At higher K's and crack speeds, the slopes increase to a range of values from 0.5 to ∞. This increase may be due to a combination of flow-controlled crack growth and crack blunting effects. Blunting effects have been observed from an examination of the fracture surface which will be discussed later. In distilled water, flow-controlled crack growth may be operative if distilled

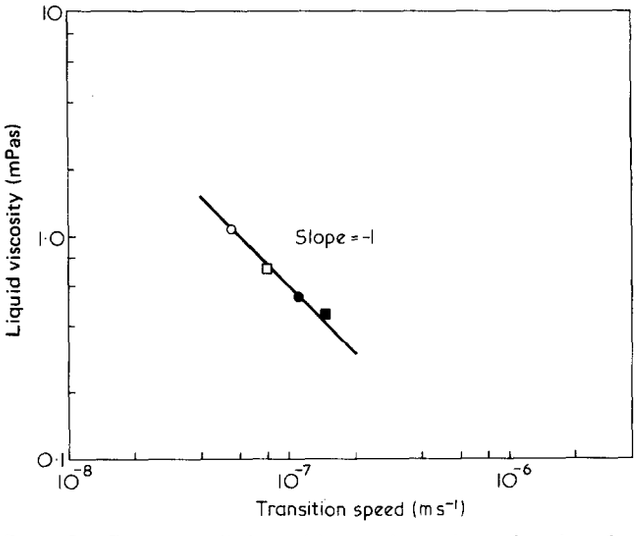

Figure 9 Flow-controlled transition crack speeds as a function of liquid viscosity for 006–60 in Comprox 2% at different temperatures: (○) +19°C; (□) +40°C; (●) +60°C; (■) +75°C. (Note logarithmic scales)

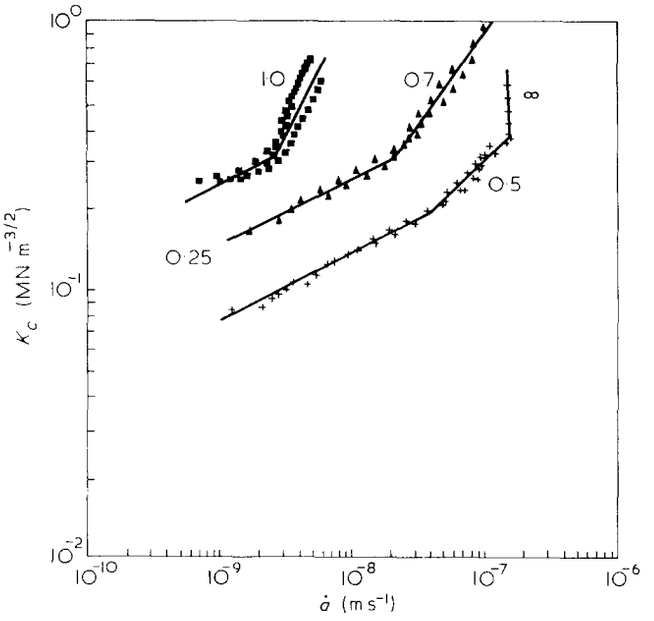

Figure 10 K_c–$\dot{a}$ curves for 002–40 in two different environments at various temperatures: (■) in distilled water at +80°C; (▲) in Comprox 2% at +60°C; (+) in Comprox 2% at +75°C. Numbers alongside curves indicate slopes of respective lines

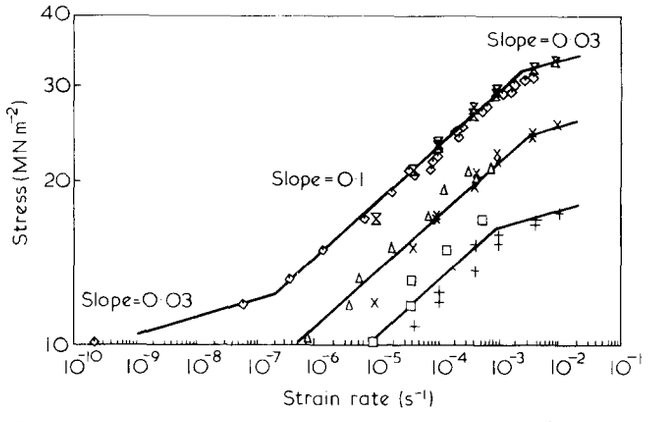

Figure 11 Creep/yield test data for 006–60 in air at +19°C for two different modes of loading at various strains. Constant load tests: (□) at 1% strain; (△) at 2% strain; (◇) at 6% strain. Constant strain rate tests: (+) at 1% strain; (x) at 2% strain; (x) at 6% strain

water is aggressive, but this is not expected and the high slope may be attributed to crack blunting effects.

Creep and yield characteristics of 006-60 in air at different temperatures

The creep and yield behaviour of 006-60 was studied in air at various temperatures corresponding to those used for the crack growth work to examine whether the crack growth behaviour (in particular, the slope of 0.25) could be related to the local viscoelastic relaxation processes at the crack tip. In *Figure 11*, the stresses at various strains are plotted as a function of strain rate on a logarithmic basis for constant load and constant strain rate tests at +19°C. It can be seen that the data for the two modes of loading can be reconciled on this basis. *Figure 12* shows the data obtained from constant strain rate tests at four temperatures plotted on a similar basis as *Figure 11*. The yield stress data determined at maximum load are shown for all four temperatures as well as the stress determined at 6% strain for some tests at +19°C and +40°C. It can be seen that the stress at 6% strain is very close to the yield stress. Hence, 6% strain may be taken as the yield strain. The yield stress data show a rate dependence, n, of about 0.1 at each temperature with n decreasing to 0.03 for low and high strain rates. At higher temperatures, these changes in slope occur at higher strain rates. The change in slope at low strain rates has been observed before[8]. The modulus determined at a fixed strain (e.g. 2% secant modulus or the modulus at yield of 6% strain) will follow approximately the same rate dependence as the yield stress, i.e. $n \simeq 0.1$ in the intermediate region and $n \simeq 0.03$ for low and high strain rates.

The temperature dependence of the yield stress and modulus can be described by an Arrhenius equation of a form similar to equation (4). Plotting ln (strain rate) *versus* $1/T$, as shown in *Figure 6*, results in an activation energy, ΔH, of 152 kJ mol^{-1}, which is about 1.5 times greater than that for 'steady' crack growth in distilled water.

Fractographic studies

As will be discussed later, it has not been possible to ratify the slope of 0.25 for crack growth by any viscoelastic analysis based on relaxation processes at the crack tip. Also, the different slopes that seem to occur in 002-40 are difficult to interpret solely from K_c–$\dot{a}$ curves. Therefore, a study of the fracture surfaces with the scanning electron microscope was undertaken to obtain important information and possible clues as to the fracture mechanisms involved. In all the micrographs shown, the direction of crack propagation is from left to right.

Figure 13 shows a series of micrographs corresponding to positions indicated on the K_c–$\dot{a}$ curve. The pictures have been taken from fractures of 006-60 in air at +19°C.

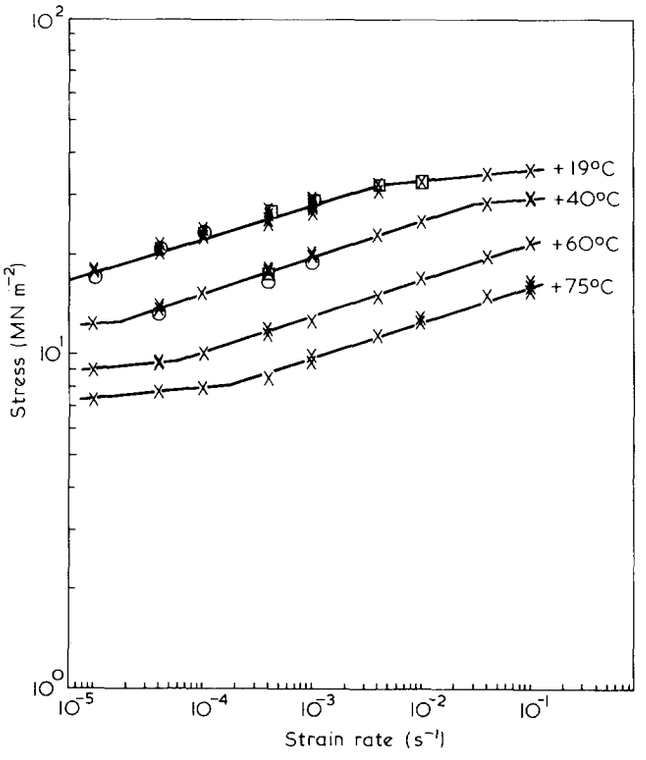

Figure 12 Constant strain rate yield data for 006–60 in air at different temperatures: (x) determined at maximum load; (○) determined at 6% strain

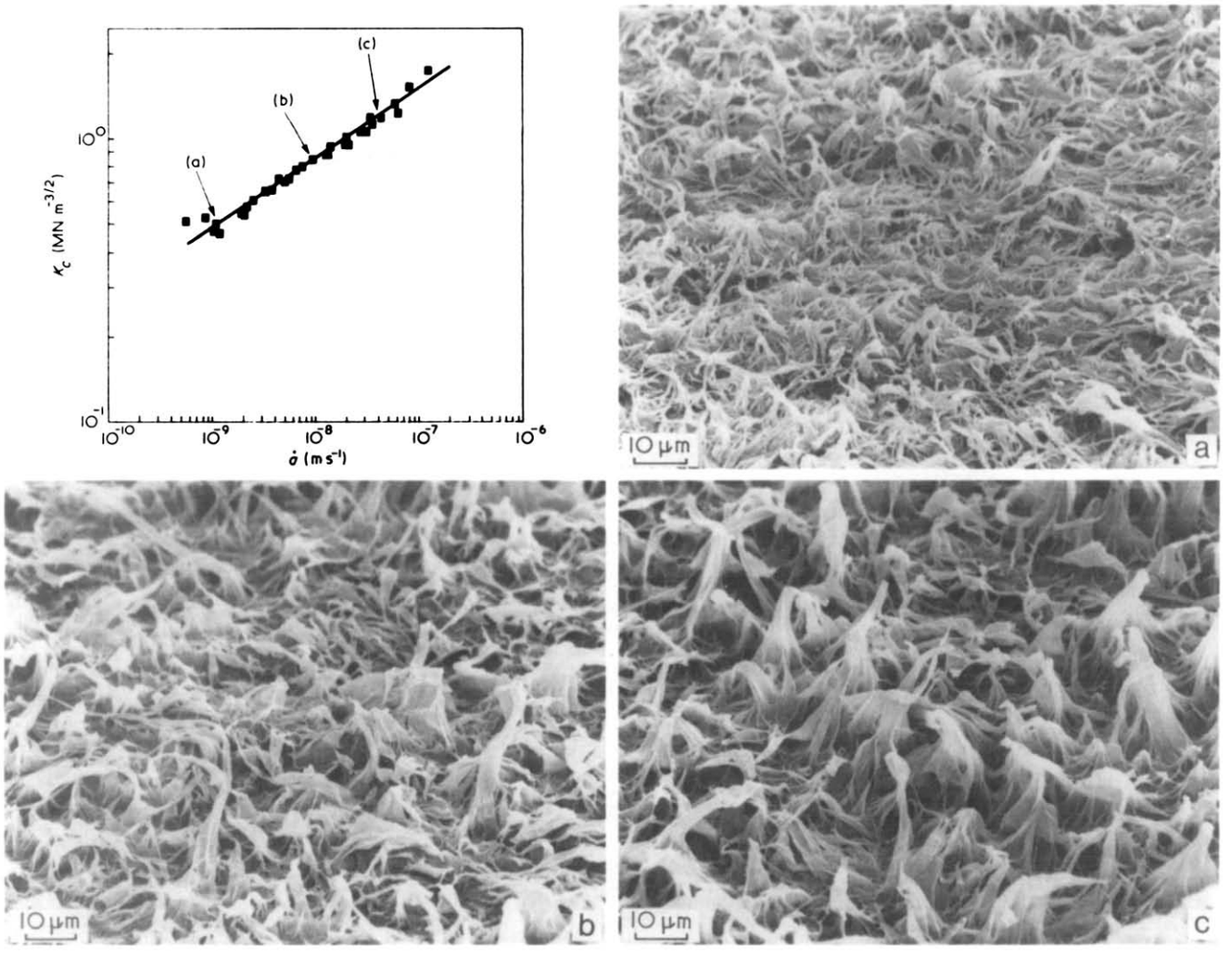

Figure 13 *SEM* micrographs of fracture surfaces of 006–60 in air at +19°C, taken at positions shown on the K_c–$\dot{a}$ curve

Fractures in distilled water do not show significant differences—the fibrils are slightly more drawn in distilled water, indicating the slight plasticization effect. It has been pointed out before that the K_c–$\dot{a}$ curves for distilled water and air at +19°C are not significantly different. This similarity is also borne out in the fracture surface appearance. From *Figure 13*, it can be seen that the fracture surfaces consist of voids and fibrils. However, the interesting observation is that the fibrillar structure increases in coarseness from low speeds (low K's) to high speeds (high K's).

Figure 14 shows a series of micrographs for fracture surfaces of 006-60 in distilled water and Comprox 2% at +75°C. The positions on the K_c–$\dot{a}$ curves where the pictures have been taken are also shown. *Figure 14d* in Comprox 2% at low K shows an unfibrillated surface with smooth conical spherulitic features of about 10 μm in size. This can be considered as interlamellar failure[9]. At the transition to flow-controlled crack growth (*Figure 14e*), the spherulitic features are still predominant with some evidence of fibril formation. As the crack growth enters into the flow-controlled regime, the smooth spherulite boundaries are quickly lost and are replaced by a completely fibrillated structure (*Figure 14f*). In the region where crack growth in detergent merges with that in distilled water, the fibrillar structures are similar (*Figures 14c* and *14g*). For distilled water, the texture of the fracture surface is predominantly fibrillar, the coarseness increasing with increasing crack speed (increasing K) as shown in *Figures 14a–c*. The only exception is that for the lowest K (*Figure 14a*), in which spherulitic features can be observed. It is worth noting that this occurs at a K value in which similar spherulitic features are observed in fractures in Comprox 2%. Evidently, below K of about 0.1 MN m$^{-3/2}$, interlamellar failure occurs, whether in detergent or in distilled water.

Figure 15 shows micrographs of fracture surfaces of 002-40 in Comprox 2% at +75°C corresponding to positions shown on the K_c–$\dot{a}$ curve. They show a much more regular array of voids and fibrils than those of 006-60. Again, the coarseness (indicated by the size of voids) increases with increasing crack speed and K. An interesting feature can be observed in *Figure 15e*, which shows a low magnification picture of the region of constant crack speed, of what appears to be a series of arrest lines. Arrest lines are indicative of stick–slip crack propagation which has been attributed to crack tip blunting effects[10].

DISCUSSION OF MECHANISMS OF FAILURE

Several mechanisms have been mentioned in the foregoing discussions, some of which have been demonstrated in previous works on slow stable crack growth in polymers[6].

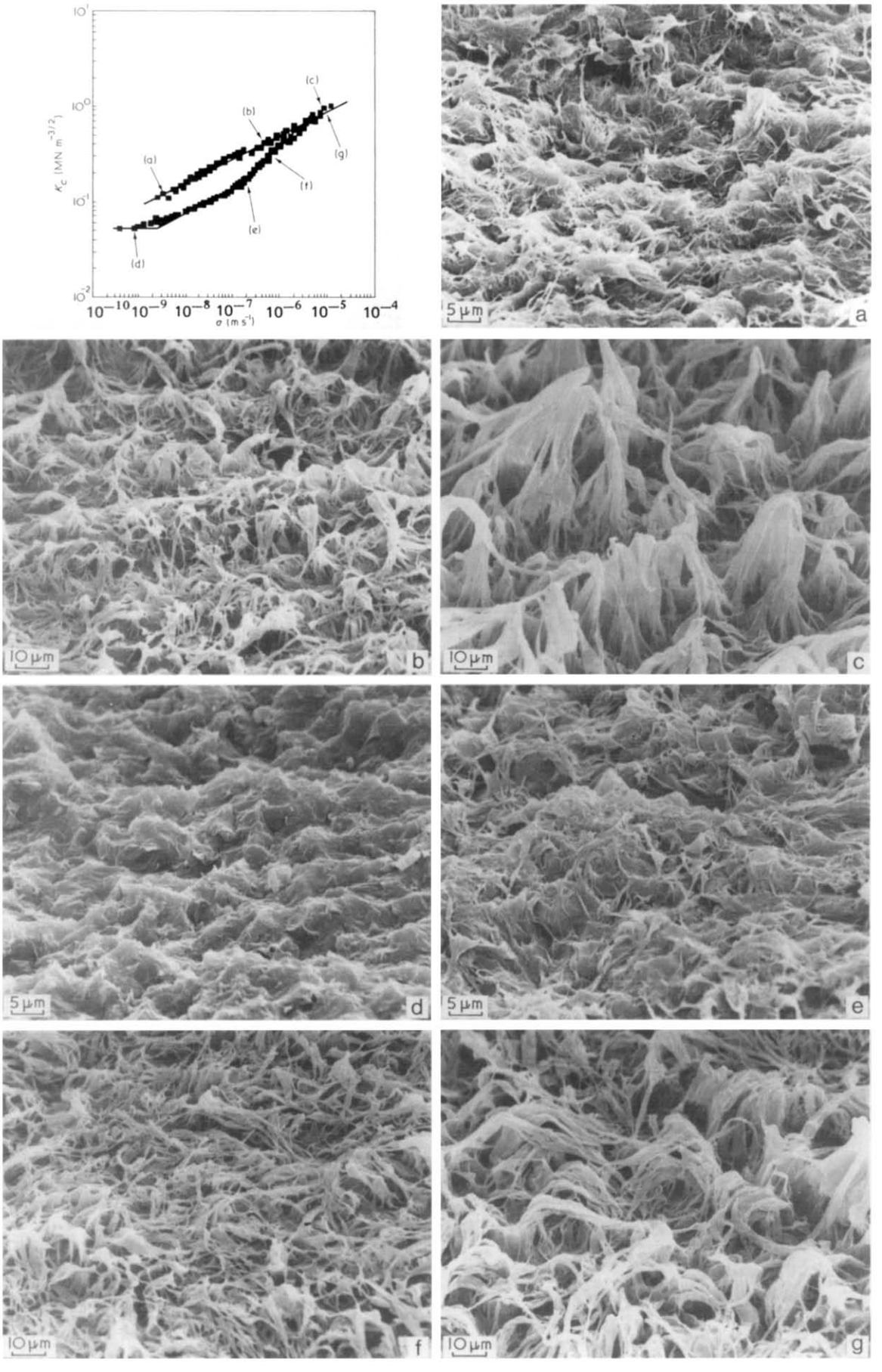

Figure 14 *SEM* micrographs of fracture surfaces of 006–60 in two different environments at +75°C, taken at positions shown on the K_c–$\dot{a}$ curves: (a) to (c) in distilled water, (d) to (g) in Comprox 2%

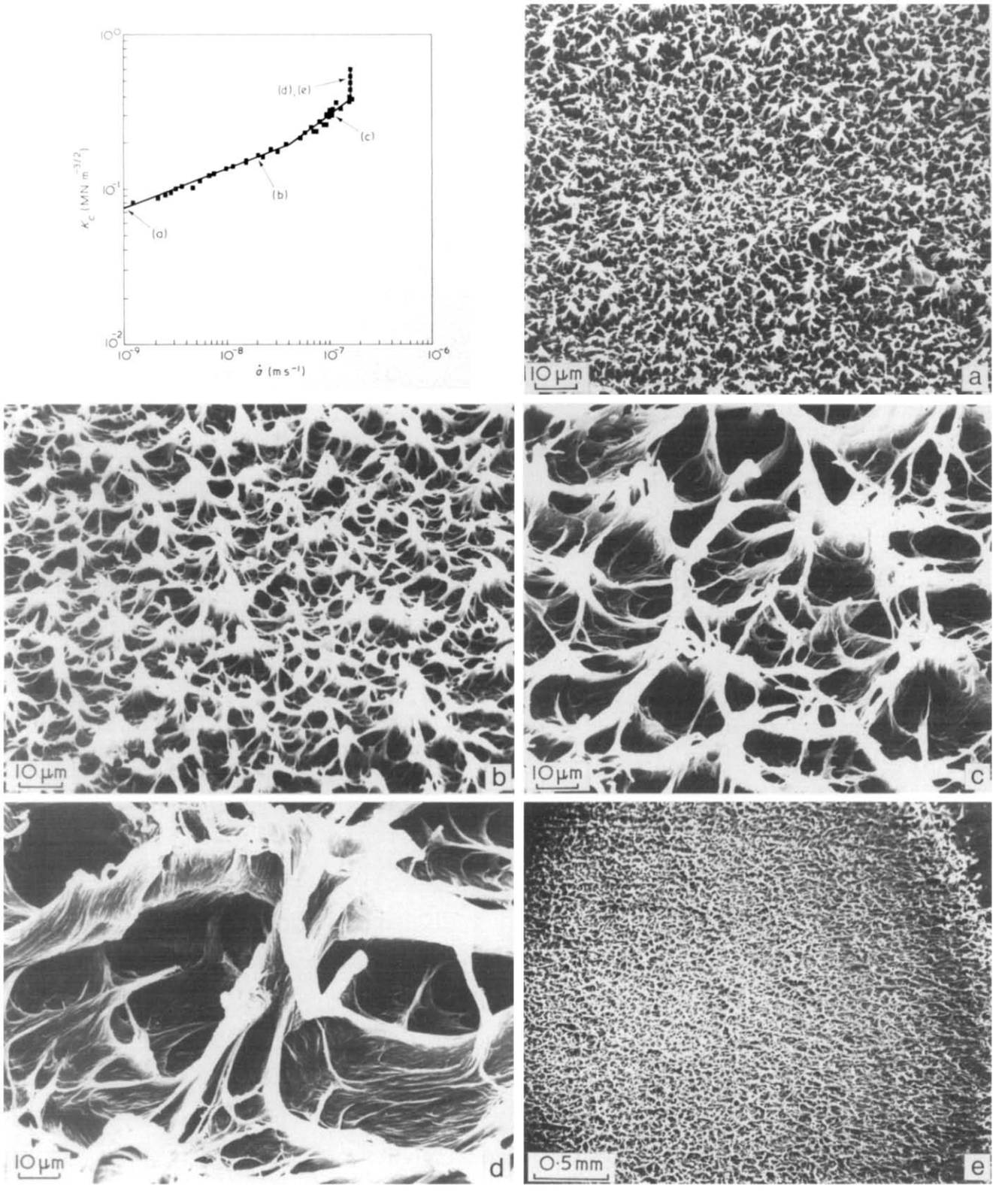

Figure 15 *SEM* micrographs of fracture surfaces of 002–40 in Comprox 2% at +75°C, taken at positions shown on the K_c–$\dot{a}$ curve

This section will deal primarily with observations that have not been explained before, in particular the time dependence of 0.25 and the high slopes encountered in fracture of 002-40.

The time dependence of 0.25 has been noted before[4] and occurs in long-term pipe failures. Relaxation-controlled crack growth based on a constant crack opening displacement criterion gives a prediction similar to the time dependence in creep and yield behaviour ($\simeq$0.1 maximum in this case). Flow-controlled crack growth applies in the presence of aggressive environments but air and distilled water have not manifested any aggressive effect in the present work. Hence, it appears that a separate mechanism is operating which cannot be explained by previous theories. A possible mechanism has been suggested[11] which will now be discussed.

The results from the fractographic studies have provided some clue as to that mechanism. The increase in coarseness of the fibrillar structure of the fracture surface from low to high speeds indicates that the number of fracture initiation sites per unit of crack area is greater at low speeds (long times) than at high speeds (short times). If it is postulated that this number, N, is diffusion-controlled following a time dependence of 0.5, then $N \propto t^{0.5} \propto \dot{a}^{-0.5}$. The site spacing, l, in inversely proportional to N, i.e. $l \propto 1/N \propto t^{-0.5} \propto \dot{a}^{0.5}$. If the fracture criterion K_c is written in terms of a local critical stress σ_c at a characteristic distance given by the site spacing l[12], then:

$$K_c = \sigma_c \sqrt{2\pi l} \propto t^{-0.25} \propto \dot{a}^{0.25} \tag{5}$$

as observed, assuming a constant σ_c for a given temperature and environment. Solid state diffusion in a polymer has been shown to influence fracture from crack healing studies in PMMA[13]. However, the precise mechanism involved here is not clear. What is observed indicates that it is void growth from a random population of sites whose initiation is inherently time-dependent, probably diffusion-controlled.

The high slopes of $n=0.5$ to ∞ encountered in the fracture of 002-40 in Comprox 2% may be partly explained by flow-controlled crack growth where $n=\frac{1}{2}$ and, in some cases, $n \rightarrow \infty$ have been modelled previously[3]. However, there is reason to believe from fractographic studies that an additional mechanism may be operating. Moreover, the high slope for fracture in distilled water cannot be attributed to flow-controlled crack growth since, as explained previously, flow-controlled applies to aggressive environments only and distilled water is not considered to be agressive for the material used here. The existence of arrest lines on the fracture surface in the high slope region, as noted in the previous section, is evident of stick–slip crack propagation. This behaviour has been observed in epoxy resins under certain conditions and has been demonstrated to be due to crack blunting effects[10]. In the present case, it is believed that the same mechanism may be operating as well. Crack blunting can lead to elevated slopes. If it is assumed that $n=0.25$ represents the sharp crack situation, then the deviation to a higher slope implies that the measured K is elevated above the K for the sharp crack case. This elevation can come from crack blunting since the effect of crack blunting is to lower the effective stress intensity at the crack tip so that the measured applied stress intensity, K_B (for the blunt crack), is apparently elevated in order to maintain the effective stress intensity at the level of the fracture criterion K_c. The effect of blunting can be represented by the following expression which relates the apparent fracture toughness, K_B, to the sharp crack fracture criterion, K_c, the crack tip radius, ρ, and a characteristic distance ahead of the tip, r_c[10]:

$$K_B = K_c \frac{(1+\rho/2r_c)^{3/2}}{(1+\rho/r_c)} \tag{6}$$

It can be shown from the above relation that when $\rho/r_c > 4$, crack blunting has a significant effect on K_B[15]. For $\rho/r_c \leqslant 4$, $K_B \simeq K_c$. When $\rho/r_c > 4$, $K_B > K_c$ and at large values of ρ, $K_B \propto \rho^{\frac{1}{2}}$.

In the crack growth studies, it is observed that the crack opening displacement (COD) increases with increasing K and crack speed. Since $\rho \propto$ COD, one can plot ρ *versus* crack speed and obtain a monotonically rising curve. It is expected, therefore, that there can be a region below a certain crack speed where $\rho \leqslant 4r_c$ and $K_B \simeq K_c$ so that crack blunting is not significant and $n=0.25$. Above this crack speed, $\rho > 4r_c$ so that $K_B > K_c$ causing the deviation from $n=0.25$ to a higher slope, as observed.

The determination of the transition point and the extent of increase in slope due to crack blunting would require accurate estimates of r_c and of ρ as it varies with K and crack speed. r_c can be measured from tests with artificially introduced blunt notches as in reference 14. Actual measurements of ρ are more difficult to obtain but the size of features on the fracture surface from scanning electron micrographs indicates that it is of the order of tens of microns.

In order to evaluate the possibility of crack blunting effects, a rough estimation of the transition point will be made here. An estimate of r_c is taken as the value of 18 μm reported for HDPE (002-55) measured from blunt notched impact tests at $+20^{\circ}$C[14] so that the transition point is predicted to occur when $\rho = 4r_c$, i.e., 76 μm. A rough estimate of ρ can be made from calculated values of COD using the crack growth data, assuming that ρ is proportional to COD. (The relation $\rho \simeq \frac{1}{2}$COD appears to be reasonable for impact tests[15].) The COD can be calculated from the commonly used expression for small-scale yielding conditions[16]:

$$\text{COD} = \frac{K_c^2}{M E \sigma_y} \tag{7}$$

where M is a constraint factor, usually between 1 and 2.

Assuming that $\rho = \frac{1}{2}$COD and replacing $E = \sigma_y/e_y$, where e_y is the yield strain ($\simeq 6\%$), we have from equation (7):

$$\rho = \tfrac{1}{2} e_y \frac{K_c^2}{M \sigma_y^2} \tag{8}$$

From equation (8), the critical value of ρ at the transition point can be estimated if K_c and σ_y are known at the transition point. From *Figure 10*, for 002-40 in distilled water at $+80^{\circ}$C, the transition point occurs at $K_c \simeq 0.3$ MN m$^{-3/2}$ which corresponds to σ_y of about 5 MN m^{-2}. Substituting these values into equation (8), we have:

$$54\ \mu\text{m} \leqslant \rho_{\text{crit}} \leqslant 108\ \mu\text{m} \quad \text{for } 1 \leqslant M \leqslant 2$$

The predicted value of 76 μm estimated previously from $\rho = 4r_c$ lies within this range. In particular, when $M=1.42$, $\rho_{\text{crit}} = 76$ μm from equation (8). A value of M of 1.42 for the constraint factor is not unreasonable. Therefore, it seems plausible that the transition point can be attributed to crack blunting effects.

The amount of increase in slope beyond the transition point (i.e. K_B/K_c) depends on the extent of crack blunting (i.e. ρ) as indicated by equation (6). Therefore, a range of slopes is compatible with the crack blunting mechanism depending on how ρ varies with K and crack speed.

More accurate estimation and definitive confirmation of these ideas can only come about through obtaining more extensive K_c–$\dot{a}$ data and additional work on ac-

curately estimating r_c and, in particular, ρ as a function of K and crack speed.

CONCLUSIONS

Fracture mechanics has been demonstrated to be a very useful tool in order to understand the basic mechanisms of slow stable crack growth in polymers, especially when combined with microscopic studies of the fracture surfaces. Two controlling mechanisms of crack growth have been observed and explained which have not been identified previously: (i) a diffusion-controlled void growith process which occurs in relatively long-term failures, and (ii) crack blunting effects which occur in relatively tough polymers. A study of incubation times and crack growth behaviour at threshold values of K using similar concepts is recommended since they may contribute to a significant portion of the failure time. An understanding of all these processes are important not only in fabricating new tougher materials, but also in designing components against long-term failure. Finally, the use of aggressive environments and elevated temperatures to rank tough materials in terms of resistance to long term failure is considered safe but conservative since such materials, which are extremely resistant to crack growth in inert environments, crack much more readily in the presence of active environments at high temperatures.

ACKNOWLEDGEMENTS

The authors wish to thank BP Chemicals Limited for the provision of materials and generous financial support of this project.

REFERENCES

1 Chan, M. K. V. and Williams, J. G. *Polym. Eng. Sci.* 1981, **21**, 1019
2 Brown, W. F. and Srawley, J. E. *ASTM STP 410* 1967, 1–65
3 Williams, J. G. in 'Advances in Polymer Science', 1978, **27**, 67, Springer-Verlag, Berlin
4 Gray, A., Mallinson, J. N. and Price, J. B. *Plast. Rubb. Proc. Appl.* 1981, **1**, 51
5 McCrum, N. G., Read, B. E. and Williams, G. 'Anelastic and Dielectric Effects in Polymeric Solids', John Wiley and Sons, New York, 1967, p 357
6 Williams, J. G. and Marshall, G. P. *Proc. Roy. Soc. London* 1975, **A342**, 55
7 Chan, M. K. V. and Williams, J. G. *Int. J. Fracture* submitted for publication
8 Wilding, M. A. and Ward, I. M. *Polymer* 1981, **22**, 870
9 Bandyopadhyay, S. and Brown, H. R. *Polymer* 1978, **19**, 589
10 Kinloch, A. J. and Williams, J. G. *J. Mater. Sci.* 1980, **15**, 987
11 Williams, J. G. and Chan, M. K. V. to be presented at the 28th IUPAC Macromolecular Symposium, University of Massachusetts, Amherst, USA, 12–15 July, 1982
12 Williams, J. G. *Metal Sci.* 1980, **14**, 344
13 Jud, K., Kausch, H. H. and Williams, J. G. *J. Mater. Sci.* 1981, **16**, 204
14 Plati, E. *PhD Thesis* Imperial College, University of London (1975)
15 Williams, J. G. and Hodgkinson, J. M. *Proc. Roy. Soc. Lond.* 1981, **A375**, 231
16 Dawes, M. G. *ASTM STP 668* 1979, p 307